DOI: 10.1002/ejic.200700056

Mixed Titanium–Hafnium Chloridometallate Complexes

Emmanuel Robé,[a] Sébastien Maria,[a] Philippe Richard,[a] and Rinaldo Poli*[b]

Keywords: Titanium / Hafnium / Chloridometallate complexes / Mixed-metal complexes

The addition of either NEt_3BzCl or $[Ph_3PNPPh_3]Cl$ (1 equiv. chloride per metal) to a 1:1 mixture of $HfCl_4$ and $TiCl_3$ in $SOCl_2$ results in Ti oxidation and leads to the corresponding salts of the $[TiHfCl_{10}]^{2-}$ ion. A solution IR investigation in the ν(M–Cl) region indicates that this ion is in equilibrium with the homodimetallic $[Ti_2Cl_{10}]^{2-}$ and $[Hf_2Cl_{10}]^{2-}$ ions. An X-ray study of the NEt_3Bz^+ salt reveals an edge-sharing bioctahedral dianion sitting on a crystallographic inversion centre. The crystal is a solid solution of different species with compositional disorder at the metal site, each metal position having the occupancy $Ti_{0.685}Hf_{0.315}$. The M–M and M–Cl distances have intermediate values between those of the homodimetallic analogues. The results of DFT calculations rationalize the structural, energetic and M–Cl bonding differences. An electrochemical investigation, in comparison with that of $[Ti_2Cl_{10}]^{2-}$ and the parallel IR studies, provides further information on the solution equilibria. Adventitious hydrolysis during the crystallization of the $[Ph_3PNPPh_3]^+$ salt affords crystals of $[Ph_3PNPPh_3]_2[Cl_3Ti(\mu\text{-}O)HfCl_5]$, whose dianion contains a tetrahedral Ti^{IV} centre and an octahedral Hf^{IV} centre bridged by an oxygen atom. A bond-length analysis allows the description of this dianion as containing the hitherto unknown $[Ti(O)Cl_3]^-$ complex, which acts as an oxygen-based donor ligand to $[HfCl_5]^-$.

Introduction

Titanium chlorides are of fundamental importance in Ziegler–Natta polymerization. The first catalyst for this process was prepared by mixing $TiCl_4$ and $AlEt_3$ or Et_2AlCl.[1–3] Other metal halides have been extensively investigated, and the literature abounds with reviews and patents on this subject, but the characterization of heterogeneous Ziegler–Natta catalysts at the atomic level is still actively pursued.[4–15] Among several improvements over the original catalyst, the use of mixed-metal systems, for instance Ti–V systems, are worth of particular mention.[16–18] Recently, mixed hafnium–titanium based catalysts have been explored as substitutes for the high-temperature polyethylene process.[19–21] To the best of our knowledge, the role played by the Hf metal has not yet been elucidated. Far from answering questions related to the structure and mechanism of the heterogeneous catalyst active sites, simple model compounds may nevertheless provide at least a basis to address the nature of the resting state of a surface active site, and the effect that a second (additive) metal may have on the ground-state properties of the first (catalytically active) one.

Only a limited number of well-defined compounds that contain both titanium and hafnium in the same molecule can be found in the literature. The only examples that we have been able to find are restricted to $(NMe_2)_2Ti(\mu\text{-}NMe_2)_2HfCl_4$,[22] $Cp_2Ti(\mu\text{-}CH_2)_2HfCp_2$,[23,24] $Cl_4Ti(\mu\text{-}C_{12}H_6N_2O_2)HfCl_4$ and $Cp_2Ti(\mu\text{-}C_{12}H_6N_2O_2)HfCl_4$ ($C_{12}H_6N_2O_2$ = 1,10-phenanthroline-5,6-dione, κ^2-*N*,*N*-coordinated to $HfCl_2$ and κ^2-*O*,*O*-coordinated to $TiCl_4$ or Cp_2Ti)[25] and two octametallic oxo- and methacrylato-bridged compounds, $Ti_4Hf_4O_6(OPr)_4(O_2CCMe{=}CH_2)_{16}$ and $Ti_2Zr_5HfO_6(O_2CCMe{=}CH_2)_{20}$,[26] the latter ones being apparently the only structurally characterized examples. Since the preparation of Ziegler–Natta catalysts is generally performed from simple, commercially available chloride compounds, it is of interest to explore mixed-metal systems where chlorides are the only available supporting ligands. In catalyst preparation, intimate mixtures or solid solutions of the metal halides are generally treated in situ with the organoaluminium activating agent, which therefore introduces alkylated active sites on the surface of the mixed-metal halide material.

In general, simple molecular chloridometallate complexes can be viewed as stabilized chunks of solid-state structures. For instance, the solid-state $HfCl_4$ structure displays hexagonal packing of chloride ions; the Hf^{4+} ions occupy 1/4 of the octahedral sites, which results in bioctahedral moieties that are arranged pairwise and share an edge or a triangular face.[27,28] The well-defined dinuclear

[a] Institut de Chimie Moléculaire de l'Université de Bourgogne, UMR-CNRS-5260, Faculté des Sciences "Mirande", Université de Bourgogne
9 Avenue Alain Savary, 21078 Dijon cedex, France
Fax: +33-561553003
E-mail: poli@lcc-toulouse.fr
[b] Laboratoire de Chimie de Coordination, UPR CNRS 8241 liée par convention à l'Université Paul Sabatier et à l'Institut National Polytechnique de Toulouse
205 Route de Narbonne, 31077 Toulouse cedex, France

$[Hf_2Cl_{10}]^{2-}$ and $[Hf_2Cl_9]^-$ complexes, described a few years ago by Calderazzo and co-workers,[29,30] may be considered to be derived from the solid-state structure of $HfCl_4$ by chopping off "Hf_2Cl_8" pieces and stabilizing them by addition of controlled amounts of additional chloride ions to the resulting unsaturations, whereas the addition of excess Cl^- leads to the mononuclear octahedral $[HfCl_6]^{2-}$ complex[31] (Scheme 1). Ti^{IV} edge-sharing and face-sharing bioctahedral analogues ($[Ti_2Cl_{10}]^{2-}$ and $[Ti_2Cl_9]^-$) also exist,[32] and we have recently reported spectroscopic evidence for the existence of $[Ti_2Cl_{11}]^{3-}$.[33] On the other hand, the neutral system is a molecular, mononuclear four-coordinate complex, $TiCl_4$, rather than an extended solid. A face-sharing bioctahedral complex, $[Ti_2Cl_9]^{3-}$, is also known for Ti^{III}.[34,35] This is related to the solid-state structure of the catalytically relevant violet $TiCl_3$, whereas hafnium analogues are not known. We set out to prepare and characterize mixed-metal (Ti,Hf) chloridometallate complexes by addition of chloride ions to a mixture of Ti and Hf chlorides in the appropriate stoichiometry and report here the results of these investigations.

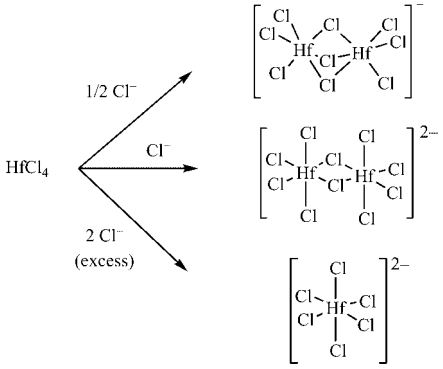

Scheme 1.

Results and Discussion

Synthetic Work

Before attempting to prepare mixed-metal complexes, we optimized the conditions for the preparation of single-metal species. Our strategy is described in Scheme 1, using the chloride salts $NEt_3Bz^+Cl^-$ and $[Ph_3PNPPh_3]^+Cl^-$ (the latter one will be abbreviated as PPN^+Cl^-). The addition of these salts to commercially available $HfCl_4$ suspended in CH_2Cl_2, however, did not result in any apparent interaction. Since this is in apparent contradiction with the literature (a decachloridodihafnate salt of the Ph_3C^+ cation has been obtained by addition of Ph_3CX to $HfCl_4$)[29] and since commercial $HfCl_4$ is typically contaminated by partially hydrolyzed oxo impurities, the reaction was then conducted in $SOCl_2$ in order to reconvert in situ any impurities to $HfCl_4$. Under these conditions the reaction takes place smoothly [Equation (1), ($Cat^+ = NEt_3Bz^+$, PPN^+)], leading to the isolation of white, analytically pure $[NEt_3Bz]_2[Hf_2Cl_{10}]$ and $[PPN]_2[Hf_2Cl_{10}]$ in excellent yields. We have also successfully used an alternative two-step procedure, consisting of the regeneration of pure $HfCl_4$ from the commercial source by treatment with $SOCl_2$ followed by reaction with Cat^+Cl^- in CH_2Cl_2. However, the direct reaction in $SOCl_2$ is a more practical procedure. After isolation, the compounds are readily soluble in dichloridomethane (the PPN salt has a significantly higher solubility). Analogous titanium complexes have been obtained and reported recently by us from the reaction of the same chloride salts with $TiCl_3$ in $SOCl_2$ [Equation (2)],[33] where the oxidation of the titanium centre occurs by intervention of the solvent as a source of chlorine atoms. Since $TiCl_3$ is more convenient to handle than $TiCl_4$ as starting compound, we have used the same strategy to access mixed-metal systems in this work. When the same reaction shown in Equation (1) and Equation (2) was carried out with a 1:1 mixture of $TiCl_3$ and $HfCl_4$, products corresponding to the expected mixed-metal $TiHfCl_{10}^{2-}$ stoichiometry were obtained in excellent yields [Equation (3), ($Cat^+ = NEt_3Bz^+$, PPN^+)]. The isolated compounds are yellow, which is the expected colour for Ti^{IV} (the $[Ti_2Cl_{10}]^{2-}$ salts are also yellow).

$$2\ HfCl_4 + 2\ Cat^+Cl^- \rightarrow Cat_2[Hf_2Cl_{10}] \quad (1)$$

$$2\ TiCl_3 + 2\ Cat^+Cl^- + 2\ \{Cl\} \rightarrow Cat_2[Ti_2Cl_{10}] \quad (2)$$

$$TiCl_3 + HfCl_4 + 2\ Cat^+Cl^- + 2\ \{Cl\} \rightarrow Cat_2[TiHfCl_{10}] \quad (3)$$

The major issue at this point is to find evidence for the existence of the mixed-metal species, as opposed to a 1:1 mixture of the homoleptic dimers, and to measure or at least estimate the position of the corresponding equilibrium [Equation (4)]. Both the homometallic and the heterodimetallic complexes are devoid of simple spectroscopic probes such as nuclei with a spin of 1/2 that would be suitable for an NMR investigation or with unpaired electrons for an EPR investigation, allowing them to be easily distinguished. The use of ^{47}Ti, ^{49}Ti, ^{177}Hf and ^{179}Hf NMR spectroscopy is unsatisfactory for compounds in which the metal centre has lower than cubic symmetry.[36,37]

$$[Ti_2Cl_{10}]^{2-} + [Hf_2Cl_{10}]^{2-} \rightleftarrows 2\ [TiHfCl_{10}]^{2-} \quad (4)$$

Infrared Characterization

Useful information was obtained from far-IR spectroscopy, which is sensitive to M–Cl modes, with samples in CH_2Cl_2 solutions in polyethylene cells. The effectiveness of this technique was previously shown for the homoleptic chloridotitanate species, in that the existence and solution-stability of the previously unknown $[Ti_2Cl_{11}]^{3-}$ ion could be unambiguously demonstrated.[33] Only the more soluble PPN^+ series of compounds gave sufficiently intense bands, and the results are shown in Figure 1. Note that the most distinct band of the PPN^+ cation at ca. 465 cm^{-1} (as measured for a PPNCl solution, Figure 1c) is seen in all spectra. A less distinct PPN^+ band at 393 cm^{-1} is also found in all other spectra, but at much higher relative intensity. How-

ever, our previous studies on the $[Ti_2Cl_{10}]^{2-}$ species have shown that adventitious hydrolytic impurities also generate a band at this frequency.[33] The relative intensity of this band varies as a function of the care with which the solutions are handled and increases when undried dichloromethane is used as solvent. All reported spectra were recorded in carefully dried solvent and all glassware and transfer syringes were silylated by rinsing with a 10% v/v chloroform solution of Me_3SiCl. However, we have been unable to completely eliminate this band. Given the extreme moisture-sensitivity of the Ti^{IV}–Cl bonds, it is possible that some hydrolysis occurred during the isolation procedure (washing and transfer into the storage ampoules). An analogous band is observed here also for the hafnium sample. This may also be a hydrolytic impurity coincidentally absorbing at the same frequency, or a real band for this complex. Anyhow, we will disregard this particular band in our conclusions.

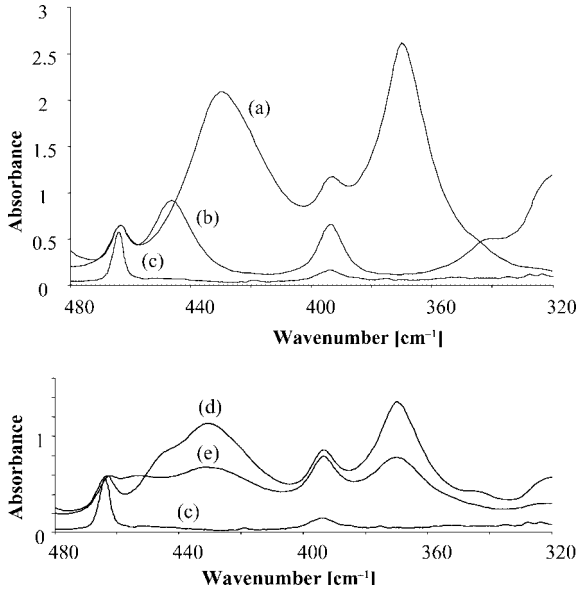

Figure 1. Far-IR spectra of PPN salts in CH_2Cl_2. All spectra are recorded at the same PPN^+ cation concentration (10^{-2} M). (a) $[PPN]_2[Ti_2Cl_{10}]$; (b) $[PPN]_2[Hf_2Cl_{10}]$; (c) [PPN]Cl; (d) electronic average of $[PPN]_2[Ti_2Cl_{10}]$ and $[PPN]_2[Hf_2Cl_{10}]$; (e) 1:1 mixture of $[PPN]_2[Ti_2Cl_{10}]$ and $[PPN]_2[Hf_2Cl_{10}]$.

$[Ti_2Cl_{10}]^{2-}$ displays two major bands at ca. 370 and 430 cm^{-1} (Figure 1a) of much stronger intensity than the band of the hafnium analogue at ca. 450 cm^{-1} (Figure 1b). The spectrum of a solution of the mixed-metal complex, at the same molar concentration of the PPN^+ cation, is shown in Figure 1e. This spectrum is identical with that obtained by mixing equimolar amounts of $Ti_2Cl_{10}^{2-}$ and $Hf_2Cl_{10}^{2-}$. This observation establishes the notion that the equilibrium shown in Equation (4) is very rapid. This spectrum shows the same maxima that are individually observed in the spectra of the two homoleptic species, and any new bands are absent. However, the overall intensity is distinctly *lower* relative to the electronic average of the spectra of the two homoleptic species (Figure 1d). The height of the peak of the PPN^+ cation at 465 cm^{-1} serves as an internal consistency check, showing the reliability of the difference between spectra (d) and (e). Since the intensity of the $[Hf_2Cl_{10}]^{2-}$ bands are so much lower than those of the corresponding titanium species, a mixed-metal analogue is likely to have intermediate intensity. Thus, the presence of some amount of the mixed-metal species is consistent with the decrease in intensity in going from the 1:1 mixture of $[Ti_2Cl_{10}]^{2-}$ and $[Hf_2Cl_{10}]^{2-}$ (Figure 1d) to the equilibrium mixture (Figure 1e). In other words, this decrease constitutes experimental evidence for the presence of mixed-metal species at equilibrium.

Structural Characterization

Single crystals have been obtained from the mixed-metal solution of the NEt_3Bz^+ salt and have been investigated by X-ray diffraction (Figure 2). Unfortunately, the compound crystallizes in a centrosymmetric space group with one half of the dianion in the asymmetric unit. Consequently, the two metal sites in the bioctahedral geometry are symmetry-disordered. Furthermore, a free occupancy refinement for the metal site as xTi + $(1 - x)$Hf gives $x = 0.685$. Therefore, the compound has excess titanium relative to the 1:1 stoichiometry. It is a solid solution containing 37% $[Ti_2Cl_{10}]^{2-}$, while the remaining 63% could be either pure $[TiHfCl_{10}]^{2-}$, or a 1:1 mixture of the Ti_2 and Hf_2 salts, or anything between these two extremes. The presence of excess titanium indicates a lower solubility for the lighter Ti_2 salt, which is then expected to shift the equilibrium of Equation (4) toward the left during the crystallization process. However, the geometrical features and the distances and angles, in comparison with those of the $[Ti_2Cl_{10}]^{2-}$ and $[Hf_2Cl_{10}]^{2-}$ anions (Table 1), are as expected and confirm the mixed-metal nature of the dianion. While the bond angles are approximately identical for the three dianions, the M–M/M′ and M–Cl bond lengths steadily increase in the order Ti_2 < $Ti_{1.37}Hf_{0.63}$ < Hf_2, as expected from the increase in the metal radius.

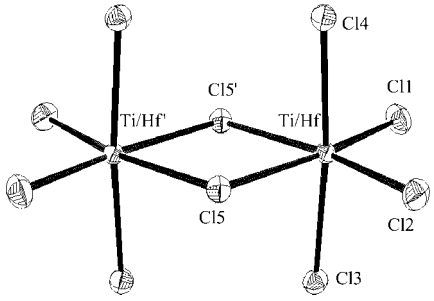

Figure 2. ORTEP view of the mixed-metal $[Ti_{1.37}Hf_{0.63}Cl_{10}]^{2-}$ anion.

Table 1. Selected bond lengths [Å] and angles [°] for the dianion in compound $[NEt_3Bz]_2[Ti_{1.37}Hf_{0.63}Cl_{10}]\cdot 2CH_2Cl_2$, and comparison with the analogous Ti_2 and Hf_2 anions.

	M = M′ = Ti [a]	MM′ = $Ti_{1.37}Hf_{0.63}$	M = M′ = Hf [b]
M–M′	3.855(3)	3.8886(4)	4.020(15)
M–Cl_{br}	2.494(13)	2.5549(6) 2.5040(6)	2.585(25)
M–Cl_{ax}	2.296(5)	2.3320(6) 2.3408(6)	2.406(13)
M–Cl_{eq}	2.258(11)	2.2929(7) 2.3028(6)	2.377(10)
Cl_{br}–M–Cl_{br}	78.78(8)	79.54(2)	78.1(1)
Cl_{br}–M–Cl_{ax}	87.9(8)	86.85(2) 87.87(2) 87.62(2) 88.71(2)	88.04(1)
Cl_{br}–M–Cl_{eq}(*cis*)	90(2)	91.54(2) 88.91(2)	90.4(4)
Cl_{br}–M–Cl_{eq}(*trans*)	169(2)	171.07(2) 168.43(2)	168.48(19)
Cl_{ax}–M–Cl_{eq}	91.7(10)	92.61(2) 92.47(2) 90.95(2) 91.40(2)	91.48(1)
Cl_{ax}–M–Cl′$_{ax}$	174.2(2)	173.95(2)	174.6(1)
Cl_{eq}–M–Cl′$_{eq}$	100.33(9)	100.02(3)	101.1(3)
M–Cl_{br}–M′	101.21(9)	100.46(2)	101.85(1)

[a] Averages of chemically equivalent values in the structure of the PCl_4^+ salt.[32] [b] Averages of chemically equivalent values in the structure of the Ph_3C^+ salt.[29]

DFT Studies

DFT calculations have been carried out on complexes $[Ti_2Cl_{10}]^{2-}$, $[TiHfCl_{10}]^{2-}$ and $[Hf_2Cl_{10}]^{2-}$ by using two different functionals (B3LYP and B3PW91) and the LANL2DZ basis set. These combinations usually give good-quality results for geometries and energies of transition-metal compounds. The calculations included a frequency analysis, and the zero-point energy, thermal and entropy corrections to give the free energies at room temperature. According to these calculations, the mixed complex is favoured relative to the mixture of the two homometallic dinuclear species by 2.04 (B3LYP) and 1.99 (B3PW91) kcal mole^{-1}, corresponding to $K \approx 30$ for the above equilibrium. More precisely, the equilibrium would consist of 13% of each of the homometallic species and 74% of the dimetallic species for a Ti/Hf ratio of 1:1. This result is in qualitative agreement with the IR results. The optimized distances (Table 2) tend to be slightly long (cf. Table 1); the B3PW91 results are closer to the experimental observations. Interestingly, whereas the M–Cl distances in the TiHf compound are, as expected, shorter for Ti than for Hf when bonded to Cl_{ax} and to Cl_{eq}, there is very little difference in the M–Cl_{br} distances involving the two different metals. This is rationalized in the next paragraph.

Table 2. Calculated bond lengths [Å] and angles [°] for $[MM'Cl_{10}]^{2-}$ (M, M′ = Ti, Hf).

	M = M' = Ti		M = Ti; M' = Hf		M = M' = Hf	
	B3LYP	B3PW91	B3LYP	B3PW91	B3LYP	B3PW91
M–M'	4.098	4.037	4.175	4.120	4.243	4.192
M–Cl_{br}	2.613	2.585	2.664	2.632	2.687	2.664
M'–Cl_{br}			2.646	2.632		
M–Cl_{ax}	2.317	2.303	2.303	2.290	2.456	2.442
M'–Cl_{ax}			2.467	2.453		
M–Cl_{eq}	2.305	2.291	2.291	2.278	2.440	2.427
M'–Cl_{eq}			2.453	2.440		
Cl_{br}–M–Cl_{br}	76.74	77.30	76.00	76.94	75.72	76.25
Cl_{br}–M'–Cl_{br}			76.61	76.95		
Cl_{br}–M–Cl_{ax}	87.51	87.40	86.26	86.25	88.34	88.22
Cl_{br}–M'–Cl_{ax}			89.49	89.20		
Cl_{br}–M–Cl_{eq}(*cis*)	91.60	91.33	91.97	91.53	92.34	92.14
Cl_{br}–M'–Cl_{eq}(*cis*)			92.06	91.85		
Cl_{br}–M–Cl_{eq}(*trans*)	168.35	168.63	167.97	168.47	168.06	168.39
Cl_{br}–M'–Cl_{eq}(*trans*)			168.67	168.80		
Cl_{ax}–M–Cl_{eq}	92.04	92.14	93.04	93.08	91.36	91.46
Cl_{ax}–M'–Cl_{eq}			90.42	90.66		
Cl_{ax}–M–Cl'$_{ax}$	171.65	173.35	170.51	170.42	175.79	175.47
Cl_{ax}–M'–Cl'$_{ax}$			178.63	177.96		
Cl_{eq}–M–Cl'$_{eq}$	100.05	100.05	100.07	100.00	99.60	99.48
Cl_{eq}–M'–Cl'$_{eq}$			99.28	90.34		
M–Cl_{br}–M'	103.25	102.70	103.70	103.05	104.28	103.75

A charge analysis (Table 3) was carried out on the B3PW91 results both at the Mulliken and at the NBO (Natural Bond Orbital) level. The latter is believed to be more descriptive for highly ionic and for weak interactions,[38] while the Mulliken analysis tends to overemphasize bond covalency. At both levels, it is clear that the Ti–Cl interactions are less polarized than the Hf–Cl interactions, as expected. The greatest difference is in the calculated charge for the bridging Cl atoms. For the TiHf compound, the calculated charges for the Cl_{ax} and Cl_{eq} atoms attached to each metal are rather close to the values of the same type of atoms in the corresponding monometallic species. The calculated charges on the Cl_{br} atoms, on the other hand, are intermediate between those of the Ti_2 and Hf_2 compounds. The result is that the Ti–Cl_{br} bond becomes more polarized (and consequently longer) in the mixed-metal complex rela-

Table 3. Mulliken and NBO charge analysis (B3PW91) for $[MM'Cl_{10}]^{2-}$ (M, M′ = Ti, Hf).

	M = M′ = Ti		M = Ti; M′ = Hf		M = M′ = Hf	
	Mulliken	NBO	Mulliken	NBO	Mulliken	NBO
M	0.2349	0.2032	0.2848	0.2187		
M′			0.5404	1.0804	0.5906	1.0877
Cl_{br}	–0. 1769	–0. 2530	–0.2354	–0.3346	–0.2829	–0.3838
Cl_{ax}(M)	–0. 2390	–0. 2321	–0.2212	–0.2112		
Cl_{ax}(M′)			–0.3343	–0.4448	–0. 3216	–0. 4316
Cl_{eq}(M)	–0.2900	–0. 24301	–0.2797	–0.2236		
Cl_{eq}(M′)			–0.3421	–0.4354	–0. 3323	–0. 4204

tive to the Ti_2 complex, whereas the Hf–Cl_{br} bond becomes less polarized (and consequently shorter) in the mixed-metal complex relative to the Hf_2 complex. Conversely, the other Ti–Cl bonds become less polarized, and the Hf–Cl more polarized, in the mixed-metal system. This charge shift introduces a permanent dipole in the dianion (Scheme 2). The variation of the Ti–Cl bond polarity may affect the performance of the catalytic site for the ethylene polymerization process.

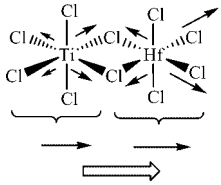

Scheme 2.

Electrochemical Investigation

A dichloromethane solution of the $[NBzEt_3]_2[TiHfCl_{10}]$ salt was investigated by cyclic voltammetry, in comparison with the analogous study reported recently for $[Ti_2Cl_{10}]^{2-}$.[33] The results are shown in Figure 3. The mixed-metal dianion exhibits a broad irreversible peak with a maximum cathode current at ca. –0.9 V vs. ferrocene, whereas the $[Ti_2Cl_{10}]^{2-}$ dianion shows two overlapping waves (a peak at ca. –1.06 V with a shoulder at ca. –0.7 V). As expected, the $[Hf_2Cl_{10}]^{2-}$ species does not exhibit any reduction process in this potential range (an irreversible reduction takes place only below –2 V).

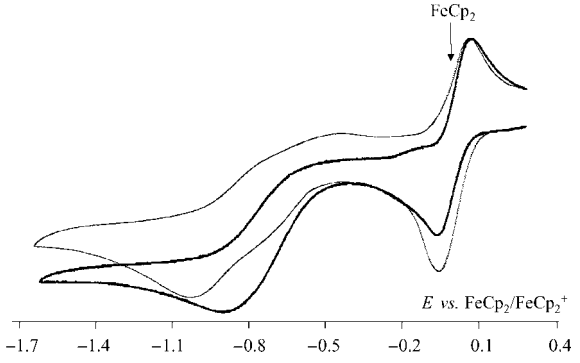

Figure 3. Cyclic voltammograms of $[NBzEt_3]_2[Ti_2Cl_{10}]$ (thinner line) and $[NBzEt_3]_2[TiHfCl_{10}]$ (thicker line). Solvent: CH_2Cl_2.

The two processes of the $[Ti_2Cl_{10}]^{2-}$ solution were shown to be related to the existence of the ligand redistribution equilibrium between the dianionic complex and complexes $[Ti_2Cl_9]^-$ and $[Ti_2Cl_{11}]^{3-}$ [Equation (5)]. Although the equilibrium is shifted to the left hand side in solution (as shown by IR spectroscopy), the easier reduction of the $[Ti_2Cl_9]^-$ ion (which is responsible for the shoulder at –0.7 V), coupled to the fast ligand redistribution process, shifts the equilibrium to the right in the diffusion layer. Thus, the peak with maximum cathode current at ca. –1.06 V is due to the reduction of the $[Ti_2Cl_{11}]^{3-}$ species. It is logical that the reduction of the latter species is placed at a more negative potential, since the positive charge density on the Ti centres is lower. The shape and position of the reduction wave for the mixed-metal dianion shows that it may correspond to a species whose charge density is similar to that of $[Ti_2Cl_9]^-$, whereas there is definitely no activity in the characteristic region of $[Ti_2Cl_{11}]^{3-}$. It is therefore rather logical to formulate the hypothesis of a similar chloride redistribution equilibrium for the mixed-metal dianion. However, because of the greater Lewis acidity of Hf^{IV} relative to Ti^{IV}, the former metal centre will preferentially form the chloride-richer species while Ti^{IV} will preferentially form the chloride-poorer species, as shown in Equation (6). Obviously, other species such as $[TiHfCl_9]^-$ may also be present in solution, given the complexity of the coupled equilibria, and contribute to the shape of the observed reduction wave.

$$2\,[Ti_2Cl_{10}]^{2-} \rightleftarrows [Ti_2Cl_9]^- + [Ti_2Cl_{11}]^{3-} \quad (5)$$

$$2\,[TiHfCl_{10}]^{2-} \rightleftarrows [Ti_2Cl_9]^- + [Hf_2Cl_{11}]^{3-} \quad (6)$$

Structure of a Partial Hydrolysis Product

With the objective of obtaining a nondisordered solid-state structure of the mixed-metal dianion, we attempted to grow crystals of the PPN^+ salt. The crystals that slowly formed, however, turned out to be $[PPN]_2[Cl_3Ti(\mu\text{-}O)HfCl_5]$. The structure of the oxo-bridged dianion is shown in Figure 4. The two metal centres are bridged by a single oxygen atom and possess different coordination geometries, tetrahedral with three terminal Cl atoms and the bridging O atom for titanium, octahedral with five terminal Cl atoms and the bridging O atom for hafnium. Therefore, the two metal centres are not disordered in this structure. The formation of this compound can be explained by a partial hydrolysis of the decachlorido mixed-metal dianion, as shown in Equation (7). The possibility that it is obtained directly from a $HfOCl_2$ impurity in $HfCl_4$ is unlikely, since the synthesis was conducted in $SOCl_2$ as solvent (see Experimental Section). Unfortunately, we did not obtain a sufficient amount of this product to carry out an analytical and spectroscopic characterization. Its formation, however, validates the notion that well-defined mixed-metal titanium-hafnium complexes may be formed with this strategy. Given the high oxophilicity of both Ti^{IV} and Hf^{IV} chlorides, it is quite possible that Ziegler–Natta catalyst precursors contain oxo-bridged dimetallic units in the bulk or on the surface, for which this complex may represent a suitable structural model. Even though partial alkylation of the catalyst occurs in the presence of the aluminium alkyl activator, the metal–chloride bonds are expected to be alkylated preferentially, and oxo ligands may be present in the active form of the catalyst.

$$[TiHfCl_{10}]^{2-} + H_2O \rightarrow [TiHf(O)Cl_8]^{2-} + 2\,HCl \quad (7)$$

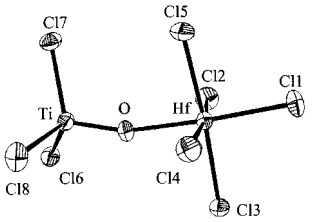

Figure 4. ORTEP view of the $[Cl_3Ti(\mu\text{-}O)HfCl_5]^{2-}$ ion.

Relevant bond lengths and angles for the $[Cl_3Ti(\mu\text{-}O)HfCl_5]^{2-}$ ion are collected in Table 4. The most interesting feature is the marked asymmetry of the oxo bridge, the Ti–O distance [1.655(4) Å] being much shorter than the Hf–O distance [2.142(3) Å]. The former is typical for terminal $Ti^{IV}O$ bond lengths, of which 25 were found in the Cambridge Structural Database (CSD), with an average value of 1.65(5) Å. There are also 7 structures in the CSD containing a Ti=O···M moiety (M = any metal). After discarding one of them (KATPUQ01), whose extremely long (> 2.1 Å) Ti=O bond length suggests a possible crystallographic problem, the remaining six bonds give an average length of 1.69(3) Å. On the other hand, the Hf–O distance is much longer than that in terminal Hf=O moieties [only one example, $(C_5Me_4Et)Hf(O)(py)$,[39] with a distance of 1.826(9) Å, has apparently been reported] and even longer than the distance of typical covalent single Hf–O bonds. For these bonds, an average of 1.97(4) Å is calculated from 148 distances found in the CSD (after excluding the values for π-delocalized donors such as carboxylates and acetylacetonates, which are significantly longer). An example where an oxygen atom bridges two metal atoms is $Cp_2(Me)Hf\text{–}O\text{–}Hf(Me)Cp_2$, with Hf–O distances of 1.941(3) Å.[40] The Hf–O distance in our ion is much closer to that of dative bonds established by neutral donors, as for instance in complex $[Hf(DMSO)_8]^{4+}$ [(2.160(12) Å].[41] Therefore, the $[Cl_3Ti(\mu\text{-}O)HfCl_5]^{2-}$ ion is best interpreted as resulting from the coordination of the hypothetical $[Ti(=O)Cl_3]^-$ anion, via a lone pair of the oxo ligand, to a $[HfCl_5]^-$ anion. Interestingly, $[TiOCl_3]^-$ does not appear to exist as an isolated species, whereas its chloride adducts $[TiOCl_4]^{2-}$ and $[TiOCl_5]^{3-}$ have been reported,[31,42–45] the former being structurally characterized as the NEt_4^+ salt (Ti–O: 1.79 Å).[46] A substructure search in the CSD for the four-coordinate Cl_3TiO moiety only reveals neutral compounds where the oxygen atom is further bonded to an alkyl, aryl or silyl group.

The Ti–Cl distances in the $[Cl_3Ti(\mu\text{-}O)HfCl_5]^{2-}$ ion average 2.232(5) Å; they are significantly longer than the average of all Ti–Cl distances in four-coordinate Cl_3TiX structures from the CSD [2.18(3) Å over 150 distances]. This is certainly related to the negative charge in this complex (formally –1 on the Ti atom), while all the literature examples are neutral complexes. The average Ti–Cl distance in the above-mentioned $[TiOCl_4]^{2-}$ ion is even longer, 2.33 Å.[46] The Hf–Cl distance *trans* to the Hf–O bond (2.4074(13) Å] is significantly shorter than the other four Hf–Cl distances, which average 2.442(9) Å. The latter compare very well with the average of all Hf–Cl distances found in all six-coordinate Cl_5HfX structures from the CSD [2.44(2) Å over 55 distances]. This is not surprising, since all CSD complexes are also anionic (monoanions with X = thf or the dinuclear $Hf_2Cl_{10}^{2-}$, or dianions of $HfCl_6^{2-}$). As expected, the distance is shorter [average of 2.302(9) Å] in the cationic complex $[(\eta^6\text{-}C_6Me_6)HfCl_3]^+$,[30] which is also formally six-coordinate from the electronic point of view. The shorter Hf–Cl1 distance in $[Cl_3Ti(\mu\text{-}O)HfCl_5]^{2-}$ indicates that the oxygen donor $[TiOCl_3]^-$ "ligand" exerts a weaker *trans* influence relative to the chloride ion.

Table 4. Selected bond lengths [Å] and angles [°] for compound $[PPN]_2[Cl_3Ti(\mu\text{-}O)HfCl_5]$.

Ti–O	1.655(4)	Hf–Cl4	2.4307(13)
Hf–O	2.142(3)	Hf–Cl5	2.4408(14)
Hf–Cl1	2.4074(13)	Ti–Cl6	2.2297(15)
Hf–Cl2	2.4520(13)	Ti–Cl7	2.2383(16)
Hf–Cl3	2.4437(12)	Ti–Cl8	2.2285(16)
Ti–O–Hf	163.0(2)	O–Hf–Cl5	85.94(10)
O–Ti–Cl6	107.21(13)	Cl1–Hf–Cl2	93.94(5)
O–Ti–Cl7	110.51(13)	Cl1–Hf–Cl3	93.02(5)
O–Ti–Cl8	108.94(13)	Cl1–Hf–Cl4	93.45(5)
Cl6–Ti–Cl7	108.01(6)	Cl1–Hf–Cl5	90.81(5)
Cl6–Ti–Cl8	110.22(6)	Cl2–Hf–Cl3	90.16(5)
Cl7–Ti–Cl8	111.84(7)	Cl2–Hf–Cl4	172.60(5)
O–Hf–Cl1	176.75(10)	Cl2–Hf–Cl5	91.04(5)
O–Hf–Cl2	85.90(10)	Cl3–Hf–Cl4	89.80(5)
O–Hf–Cl3	90.23(10)	Cl3–Hf–Cl5	175.90(5)
O–Hf–Cl4	86.70(10)	Cl4–Hf–Cl5	88.50(5)

Conclusions

This work has explored the existence and relative stability of mixed-metal Ti–Hf chloridometallate complexes, focusing on the edge-sharing bioctahedral system, $[MM'Cl_{10}]^{2-}$ (M, M′ = Ti, Hf). We have provided evidence (by a combination of low-energy IR, X-ray crystallography, DFT calculations and cyclic voltammetry) that the mixed-metal system $[TiHfCl_{10}]^{2-}$ does exist and that it is thermodynamically more stable by a small amount than the equivalent 1:1 mixture of the homodinuclear complexes, $[Ti_2Cl_{10}]^{2-}$ and $[Hf_2Cl_{10}]^{2-}$. The comparison with the previously reported electrochemical behaviour of $[Ti_2Cl_{10}]^{2-}$ suggests a stronger preference for the Ti_2 complex to lose one Cl^- ligand, yielding $[Ti_2Cl_9]^-$, and a corresponding stronger preference for the Hf_2 complex to add one more Cl^- ligand, yielding $[Hf_2Cl_{11}]^{3-}$. A partial hydrolysis product obtained from the above mixture is an unprecedented mixed Ti–Hf chloridometallate ion, $[Cl_3Ti(\mu\text{-}O)HfCl_5]^{2-}$, the structure of which is best interpreted as an octahedral $[HfCl_5X]^{2-}$ complex where X is the previously unknown tetrahedral $[Cl_3Ti(O)]^-$ ion. The oxygen atom that bridges the two metals is doubly bonded to the Ti centre and donates a lone pair to the Hf centre.

Experimental Section

General Procedures: All preparations and manipulations were carried out with Schlenk techniques under an oxygen-free argon atmo-

sphere. All glassware was oven-dried at 120 °C. For particular applications (see Results and Discussion) it was silylated by being washed with a $CHCl_3$ solution of Me_3SiCl (10% v/v). Solvents were dried by standard procedures and distilled under dinitrogen prior to use.

Materials: CH_2Cl_2 was purified by reflux and distillation over P_4O_{10} under argon. Pentane was purified by reflux over sodium benzophenone ketyl and distilled under argon. $TiCl_3$, $HfCl_4$ and the chloride salts triethylbenzylammonium chloride, $[NEt_3Bz]Cl$, and bis(triphenylphosphanyl)iminium chloride, [PPN]Cl, were purchased from Aldrich and used as received. Complexes $[NEt_3Bz]_2[Ti_2Cl_{10}]$ and $[PPN]_2[Ti_2Cl_{10}]$ were prepared as recently described.[33]

Instrumentation: The infrared spectra were recorded with a Bruker Vector 22 instrument equipped with a Globar (MIR) source. The solution spectra in the far-IR (480–300 cm^{-1}) region were obtained from CH_2Cl_2 solutions in polyethylene cells (0.5 mm path length). Cyclic voltammograms were recorded with an EG&G 362 potentiostat connected to a Macintosh computer through MacLab hardware/software. The electrochemical cell was fitted with an Ag/AgCl reference electrode, a platinum disk working electrode and a platinum wire counterelectrode. $[Bu_4N]PF_6$ (ca. 0.1 M) was used as supporting electrolyte in thf. All potentials are reported relative to the ferrocene standard, which was added to each solution and measured at the end of the experiments. Elemental analyses were carried out with a Fisons EA 1108 instrument by the analytical services of LSEO.

Preparation of $[NEt_3Bz]_2[Hf_2Cl_{10}]$: A Schlenk tube was charged with $HfCl_4$ (1.161 g, 3.62 mmol) and $[NEt_3Bz]Cl$ (0.826 g, 3.62 mmol). Thionyl chloride (10 mL) was added by syringe under magnetic stirring and the apparatus was connected to an oil bubbler. *Warning: The reaction between $SOCl_2$ and water (potentially present as a contaminant in the starting salts) produces toxic SO_2 and HCl; therefore, the reaction must be carried out under a well-ventilated fume hood.* A white suspension was observed. The reaction mixture was heated to 65 °C for 1 h in an oil bath and then cooled to room temperature. After stirring for 1 h at room temperature, pentane (20 mL) was added, causing the precipitation of the product as a white powder. After being filtered, the solid was washed with pentane and dried under vacuum overnight. Yield: 1.858 g (94%). $C_{26}H_{44}Cl_{10}Hf_2N_2$ (1096.14): calcd. C 28.5, H 4.0, N 2.6; found C 27.8, H 4.2, N 2.7.

Preparation of $[PPN]_2[Hf_2Cl_{10}]$: By following a procedure identical to that described above for $[NEt_3Bz]_2[Hf_2Cl_{10}]$, $[PPN]_2[Hf_2Cl_{10}]$ (3.292 g, 92%) was obtained starting from $HfCl_4$ (1.994 g, 6.23 mmol) and PPNCl (3.570 g, 6.23 mmol). $C_{72}H_{60}Cl_{10}Hf_2N_2P_4$ (1788.66): calcd. C 48.4, H 3.4, N 1.6; found C 48.1, H 3.4, N 1.8.

Preparation of $[NEt_3Bz]_2[TiHfCl_{10}]$: A Schlenk tube was charged with $HfCl_4$ (1.688 g, 5.27 mmol), $TiCl_3$ (0.809 g, 5.25 mmol) and $[NEt_3Bz]Cl$ (2.392 g, 10.50 mmol). Thionyl chloride (50 mL) was

Table 5. Crystal data and structure refinement for both compounds.

Compound	$[NEt_3Bz]_2[Ti_{1.37}Hf_{0.63}Cl_{10}]\cdot 2CH_2Cl_2$	$[PPN]_2[Cl_3Ti(\mu\text{-}O)HfCl_5]$
Formula	$C_{28}H_{48}Cl_{14}Hf_{0.63}N_2Ti_{1.37}$	$C_{72}H_{60}Cl_8HfN_2OP_4Ti$
M_r	1087.01	1603.09
T [K]	110(2)	110(2)
Crystal system	triclinic	monoclinic
Space group	$P\bar{1}$	$P2_1/c$
a [Å]	7.6739(2)	25.7548(5)
b [Å]	10.9860(2)	12.8363(2)
c [Å]	14.2333(4)	21.1674(3)
α [°]	108.938(1)	90.0
β [°]	97.971(1)	78.562(1)
γ [°]	104.494(1)	90.0
V [Å]^3	1066.72(5)	6858.9(2)
Z	1	4
$F(000)$	543.5	3216
D_{calc} [g cm^{-3}]	1.692	1.552
Diffractometer	Nonius KappaCSD	Nonius KappaCSD
Scan type	&πηι; rot. and ψ scans	&πηι; rot. and ψ scans
λ [Å]	0.71073	0.71073
μ [mm^{-1}]	2.69	2.08
Crystal size [mm^3]	$0.45\times0.20\times0.05$	$0.37\times0.25\times0.15$
$\sin(\theta)/\lambda$ max [Å^{-1}]	0.65	0.65
Index ranges	h:–9; 9	h:–33; 32
	k:–14; 13	k:–16; 13
	l:–18; 18	l:–27; 27
RC = Refl. Collected	8402	38133
IRC = independent RC	4787 [R(int) = 0.032]	15599 [R(int) = 0.058]
IRCGT = IRC and [$I>2\sigma(I)$]	4253	10420
Refinement method	Full-matrix L.S. on F^2	Full-matrix L.S. on F^2
Data/restraints/param.	4787/0/210	15599/0/802
R for IRCGT	R_1[a] = 0.033, wR_2[b] = 0.081	R_1[a] = 0.051, wR_2[b] = 0.112
R for IRC	R_1[a] = 0.039, wR_2[b] = 0.084	R_1[a] = 0.095, wR_2[b] = 0.126
Goodness-of-fit[c]	1.042	1.033
$\Delta\rho$, max, min [e Å^{-3}]	0.764 and –1.122	2.22 and –1.26

[a] $R_1 = \Sigma\,(||F_o| - |F_c||)/\Sigma|F_o|$. [b] $wR_2 = [\Sigma w(F_o^2 - F_c^2)^2/\Sigma\,[w(F_o^2)^2]^{1/2}$ where $w = 1/[\sigma^2(F_o^2 + (0.046P)^2 + 0.37P]$ for $[NEt_3Bz]_2[Ti_{1.37}Hf_{0.63}Cl_{10}]$ and $w = 1/[\sigma^2(F_o^2 + (0.060P)^2 + 0.86P]$for $[PPN]_2[Cl_3Ti(\mu\text{-}O)HfCl_5]$ where $P = (\mathrm{Max}(F_o^2,0) + 2*F_c^2)/3$. [c] Goodness of fit = $[\Sigma w(F_o^2 - F_c^2)^2/(N_o - N_v)]^{1/2}$.

added by syringe under magnetic stirring, and the apparatus was connected to an oil bubbler. A dark purple suspension was observed. The reaction mixture was refluxed for 1 h in an oil bath. The dark-purple suspension transformed gradually into a yellow solution. It was then cooled to room temperature and stirred for two hours. Thionyl chloride was partially removed under vacuum until a precipitate began to form. Pentane (20 mL) was then added to complete the precipitation of the product as a yellow powder. After being filtered, the solid was washed with pentane and dried under vacuum for two hours. Yield: 4.587 g (94%) $C_{26}H_{44}Cl_{10}HfN_2Ti$ (965.52): calcd. C 32.3, H 4.6, N 2.9; found C 32.1, H 4.6, N 2.9.

Preparation of $[PPN]_2[TiHfCl_{10}]$: By following a procedure identical to that described above for $[NEt_3Bz]_2[TiHfCl_{10}]$, $[PPN]_2[TiHfCl_{10}]$ (2.463 g, 94%) was obtained starting from $HfCl_4$ (0.506 g, 1.58 mmol), $TiCl_3$ (0.244 g, 1.58 mmol) and PPNCl (1.816 g, 3.16 mmol). $C_{72}H_{60}Cl_{10}HfN_2P_4Ti$ (1658.03): calcd. C 52.2, H 3.6, N 1.7; found C 53.0, H 3.6, N 2.0.

X-ray Diffraction Studies: Intensity data for both compounds were collected with a Nonius Kappa CSD at 110 K. The structures were solved by a Patterson search program and refined with full-matrix least-squares methods based on F^2 (SHELXL-97)[47] with the aid of the WINGX program.[48] All non-hydrogen atoms were refined with anisotropic thermal parameters. Hydrogen atoms were included in their calculated positions and refined with a riding model. The $[Ti_xHf_{2-x}Cl_{10}]^{2-}$ dimetallic complex is located on a centre of inversion; as a consequence, the two metal atoms are disordered and occupy the same crystallographic position. Furthermore, the two metal atoms are not in a 1:1 ratio, the occupation factors converged to $m_1 = 0.685$ for the Ti atom and $m_2 = 1 - m_1$ for the Hf atom. A first attempt to refine independently both metallic positions lead to a nonrealistic result; therefore, the two positions and the anisotropic displacement parameters where constrained to be identical for both metallic centres. The molecules were drawn with ORTEP32.[49] Crystal data and refinement parameters are shown in Table 5.

CCDC-633154 and CCDC-633155 contain the supplementary crystallographic data for this paper. These data can be obtained free of charge from The Cambridge Crystallographic Data Centre via www.ccdc.cam.ac.uk/data_request/cif.

Computational Details: Calculations were carried out with the Gaussian 03 package[50] at the DFT level by means of either the B3LYP[51–53] or the B3PW91[54,55] functional and the LANL2DZ basis set.[56] All geometries were fully optimized without symmetry restrictions and were characterized as local minima of the potential energy surface (PES) by inspection of the sign of the second derivatives obtained from frequency calculations. The Gibbs free energies were obtained after correction for the ZPVE, PV and TS terms under the ideal gas approximation. The temperature used was 298.15 K.

Acknowledgments

We are grateful to the CNRS for support of this work.

[1] K. Ziegler, E. Holzkamp, H. Breil, H. Martin, *Angew. Chem.* **1955**, *67*, 541–547.
[2] K. Ziegler, *Nobel lecture*, http://nobelprize.org/nobel_prizes/chemistry/laureates/1963/ziegler-lecture.html, **1963**.
[3] G. Natta, *Nobel lecture*, http://nobelprize.org/nobel_prizes/chemistry/laureates/1963/natta-lecture.html, **1963**.
[4] P. Corradini, G. Guerra, L. Cavallo, *Acc. Chem. Res.* **2004**, *37*, 231–241.
[5] M. Chang, X. Liu, P. J. Nelson, G. R. Munzing, T. A. Gegan, Y. V. Kissin, *J. Catal.* **2006**, *239*, 347–353.
[6] N. Cui, Y. Ke, H. Li, Z. Zhang, C. Guo, Z. Lv, Y. Hu, *J. Appl. Polym. Sci.* **2006**, *99*, 1399–1404.
[7] Q. Wang, N. Murayama, B. Liu, M. Terano, *Macromol. Chem. Phys.* **2005**, *206*, 961–966.
[8] M. Seth, T. Ziegler, *Macromolecules* **2004**, *37*, 9191–9200.
[9] B. Liu, T. Nitta, H. Nakatani, M. Terano, *Macromol. Symp.* **2004**, *213*, 7–18.
[10] G. Kwag, J.-G. Lee, C. Bae, S. N. Lee, *Polymer* **2003**, *44*, 6555–6558.
[11] B. Liu, T. Nitta, H. Nakatani, M. Terano, *Macromol. Chem. Phys.* **2003**, *204*, 395–402.
[12] B. Liu, T. Nitta, H. Nakatani, M. Terano, *Macromol. Chem. Phys.* **2002**, *203*, 2412–2421.
[13] M. Seth, P. M. Margl, T. Ziegler, *Macromolecules* **2002**, *35*, 7815–7829.
[14] H. Weiss, M. Boero, M. Parrinello, *Macromol. Symp.* **2001**, *173*, 137–147.
[15] V. P. Oleshko, P. A. Crozier, R. D. Cantrell, A. D. Westwood, *Macromol. Rapid Commun.* **2001**, *22*, 34–40.
[16] I. Jaber, S. J. Brown, *Patent Appl. 99–304060* [assigned to Nova Chemicals (International) S. A., Switzerland], **2000**.
[17] A. Greco, G. Perego, M. Cesari, S. Cesca, *J. Appl. Polym. Sci.* **1979**, *23*, 1319–1332.
[18] F. Calderazzo, G. Pampaloni, F. Masi, A. Moalli, R. Invernizzi, *Patent Appl. 89–202199* (assigned to Enichem Anic S. p. A., Italy), **1990**, 9 pp.
[19] F. Masi, S. Malquori, L. Barazzoni, C. Ferrero, A. Moalli, F. Menconi, R. Invernizzi, N. Zandona, A. Altonmare, F. Ciardelli, *Makromol. Chem. Suppl.* **1989**, *15*, 147–165.
[20] T. Tanaka, E. Tanaka, *WO1980JP00006* (Assigned to Mitsubishi Chem. Ind.), **1980**.
[21] F. Menconi, G. Conti, A. Zanellato, A. Moalli, *US6723809* (assigned to Polimeri Europa SRL), **2004**.
[22] S. R. Wade, M. G. H. Wallbridge, G. R. Willey, *J. Chem. Soc., Dalton Trans.* **1982**, 271–274.
[23] B. J. J. Van De Heisteeg, G. Schat, O. S. Akkerman, F. Bickelhaupt, *Organometallics* **1985**, *4*, 1141–1142.
[24] B. J. J. Van De Heisteeg, G. Schat, O. S. Akkerman, F. Bickelhaupt, *J. Organomet. Chem.* **1986**, *308*, 1–10.
[25] F. Calderazzo, F. Marchetti, G. Pampaloni, V. Passarelli, *J. Chem. Soc., Dalton Trans.* **1999**, 4389–4396.
[26] S. Gross, G. Kickelbick, M. Puchberger, U. Schubert, *Monatsh. Chem.* **2003**, *134*, 1053–1063.
[27] R. Niewa, H. Jacobs, *Z. Kristallogr.* **1995**, *210*, 687.
[28] L. B. Serezhkina, V. N. Serezhkin, R. L. Davidovich, *Russ. J. Coord. Chem.* **2000**, *26*, 18–22.
[29] F. Calderazzo, P. Pallavicini, G. Pampaloni, P. F. Zanazzi, *J. Chem. Soc., Dalton Trans.* **1990**, 2743–2746.
[30] F. Calderazzo, I. Ferri, G. Pampaloni, S. Troyanov, *J. Organomet. Chem.* **1996**, *518*, 189–196.
[31] J. E. D. Davies, D. A. Long, *J. Chem. Soc. A* **1968**, 2560–2564.
[32] T. J. Kistenmacher, G. D. Stucky, *Inorg. Chem.* **1971**, *10*, 122–132.
[33] E. Robé, J.-C. Daran, S. Vincendeau, R. Poli, *Eur. J. Inorg. Chem.* **2004**, 4108–4114.
[34] P. C. Crouch, G. W. A. Fowles, R. A. Walton, *J. Chem. Soc. A* **1969**, 972–976.
[35] B. Briat, O. Kahn, I. Morgensternbadarau, J. C. Rivoal, *Inorg. Chem.* **1981**, *20*, 4193–4200.
[36] N. Hao, B. Sayer, G. Denes, D. Bickley, C. Detellier, M. Mcglinchey, *J. Magn. Reson.* **1982**, *50*, 50–63.
[37] R. T. Carlin, R. A. Osteryoung, J. S. Wilkes, J. Rovang, *Inorg. Chem.* **1990**, *29*, 3003–3009.
[38] A. E. Reed, L. A. Curtiss, F. Weinhold, *Chem. Rev.* **1988**, *88*, 899–926.

[39] W. A. Howard, G. Parkin, *J. Organomet. Chem.* **1994**, *472*, C1–C4.
[40] F. R. Fronczek, E. C. Baker, P. R. Sharp, K. N. Raymond, H. G. Alt, M. D. Rausch, *Inorg. Chem.* **1976**, *15*, 2284–2289.
[41] C. Hagfeldt, V. Kessler, I. Persson, *Dalton Trans.* **2004**, 2142–2151.
[42] A. Feltz, *Z. Anorg. Allg. Chem.* **1965**, *334*, 242–249.
[43] A. Feltz, *Z. Chem.* **1967**, *7*, 158.
[44] H. Linga, Z. Stojek, R. A. Osteryoung, *J. Am. Chem. Soc.* **1981**, *103*, 3754–3760.
[45] I. W. Sun, E. H. Ward, C. L. Hussey, *Inorg. Chem.* **1987**, *26*, 4309–4311.
[46] W. Haase, H. Hoppe, *Acta Crystallogr., Sect. B* **1968**, *24*, 282–283.
[47] G. M. Sheldrick, *SHELXL97. Program for Crystal Structure Refinement*, University of Göttingen, Göttingen, Germany, **1997**.
[48] L. J. Farrugia, *J. Appl. Crystallogr.* **1999**, *32*, 837–838.
[49] L. J. Farrugia, *J. Appl. Crystallogr.* **1997**, *32*, 565.
[50] M. J. Frisch, G. W. Trucks, H. B. Schlegel, G. E. Scuseria, M. A. Robb, J. R. Cheeseman, J. Montgomery, J. A., T. Vreven, K. N. Kudin, J. C. Burant, J. M. Millam, S. S. Iyengar, J. Tomasi, V. Barone, B. Mennucci, M. Cossi, G. Scalmani, N. Rega, G. A. Petersson, H. Nakatsuji, M. Hada, M. Ehara, K. Toyota, R. Fukuda, J. Hasegawa, M. Ishida, T. Nakajima, Y. Honda, O. Kitao, H. Nakai, M. Klene, X. Li, J. E. Knox, H. P. Hratchian, J. B. Cross, C. Adamo, J. Jaramillo, R. Gomperts, R. E. Stratmann, O. Yazyev, A. J. Austin, R. Cammi, C. Pomelli, J. W. Ochterski, P. Y. Ayala, K. Morokuma, G. A. Voth, P. Salvador, J. J. Dannenberg, V. G. Zakrzewski, S. Dapprich, A. D. Daniels, M. C. Strain, O. Farkas, D. K. Malick, A. D. Rabuck, K. Raghavachari, J. B. Foresman, J. V. Ortiz, Q. Cui, A. G. Baboul, S. Clifford, J. Cioslowski, B. B. Stefanov, G. Liu, A. Liashenko, P. Piskorz, I. Komaromi, R. L. Martin, D. J. Fox, T. Keith, M. A. Al-Laham, C. Y. Peng, A. Nanayakkara, M. Challacombe, P. M. W. Gill, B. Johnson, W. Chen, M. W. Wong, C. Gonzalez, J. A. Pople, *Gaussian 03, Revision C.02*, Gaussian, Inc., Wallingford CT, **2004**.
[51] A. D. Becke, *J. Chem. Phys.* **1993**, *98*, 5648–5652.
[52] C. T. Lee, W. T. Yang, R. G. Parr, *Phys. Rev. B* **1988**, *37*, 785–789.
[53] P. Stephens, F. Devlin, C. Chabalowski, M. Frisch, *J. Phys. Chem.* **1994**, *98*, 11623–11627.
[54] J. P. Perdew, *Phys. Rev. B: Condens. Matter* **1986**, *33*, 8822–8824.
[55] K. Burke, J. P. Perdew, Y. Wang, *Electronic Density Functional Theory: Recent Progress and New Directions* (Eds.: J. F. Dobson, G. Vignale, M. P. Das), Plenum Press, New York, **1998**.
[56] P. J. Hay, W. R. Wadt, *J. Chem. Phys.* **1985**, *82*, 270–283.

Received: January 17, 2007
Published Online: April 25, 2007

